


Spatial patterns of eastern Mediterranean climate influence on tree growth

The Holocene
2014, Vol. 24(4) 381–392
© The Author(s) 2014
Reprints and permissions:
sagepub.co.uk/journalsPermissions.nav
DOI: 10.1177/0959683613518594
hol.sagepub.com


Ramzi Touchan,¹ Kevin J Anchukaitis,² Vladimir V Shishov,³ Fatih Sivrikaya,⁴ Jihad Attieh,⁵ Muzaffer Ketmen,⁶ Jean Stephan,⁷ Ioannis Mitsopoulos,⁸ Andreas Christou⁹ and David M Meko¹

Abstract

The first large-scale network of 79 tree-ring chronologies in the Eastern Mediterranean and Near East (EMNE; 33°N–42°N, 21°E–43°E) is described and analyzed to identify the seasonal climatic signal in indices of annual ring width. Correlation analysis and cluster analysis are applied to tree-ring data and gridded climate data to assess the climate signal embedded in the network in preparation for climate field reconstructions and formal proxy/model intercomparison experiments. The lengths of the 79 combined chronologies range from 89 to 990 years. The monthly correlations and partial correlations reveal a pervasive positive association with May, June, and sometimes July precipitation, positive correlations with winter and spring (December through April) temperatures, and negative relationships with May through July temperature, although as expected, there are site-to-site exceptions to these general patterns. Cluster analysis suggests three groups of sites based on their association with climate. The chronologies for the EMNE have coherent seasonal precipitation and temperature signals across a fairly broad geographical domain. The predominant signal is a positive growth response to May–June precipitation. Collectively, the findings suggest that the network can be exploited to develop season-specific field reconstructions of precipitation and drought history in the EMNE.

Keywords

cluster analysis, correlation analysis, expressed population signal, general circulation models, tree-ring

Received 25 July 2013; revised manuscript accepted 28 November 2013

Introduction

The Eastern Mediterranean and Near East (EMNE) region is influenced by multiple local and remote climate processes. The region is exposed to the distal influences of the Asian Monsoon (Raicich et al., 2003; Rodwell and Hoskins, 1996) and the proximal effects of the East Atlantic Jet (Duenkeloh and Jacobeit, 2003; Touchan et al., 2005b; Xoplaki et al., 2004) in summer. The Siberian High Pressure System (e.g. Xoplaki et al., 2001) and North Atlantic Oscillation (Corte-Real et al., 1995; Duenkeloh and Jacobeit, 2003; Xoplaki et al., 2004) also influence regional climate. A semi-objective classification of daily synoptic maps identified no fewer than six large synoptic groups important to climatic variation in the eastern Mediterranean: Cyprus lows, the Persian trough, the Red Sea trough, Sharav lows, and Siberian/subtropical highs (Alpert et al., 2004). Precipitation trends in the last half of the 20th century appear to be related to changes in the frequency or annual number of days of these synoptic types, notably the Cyprus lows and Red Sea trough (Alpert et al., 2004). Orography and land-sea interactions (including distance from the sea) and smaller scale processes (Lolis et al., 1999; Xoplaki et al., 2001, 2003a, 2003b, 2004) are also important and can control local-scale pattern climate heterogeneity. Mediterranean climate is further influenced by the Mediterranean Sea itself (e.g. Mariotti et al., 2002; Trigo et al., 1999), which represents an important source of energy and moisture for cyclone development. Furthermore, the complex land topography around the Mediterranean plays a crucial role in steering airflow (e.g. Bartzokas et al., 1994;

Trigo et al., 1999). Perhaps, as a consequence of these multiple and superimposed influences, hydrologic variability spans a broad range of timescales and is unlikely to be fully described by the modern instrumental record. Meanwhile, the population of the eastern Mediterranean grows by 3.5% annually, while irrigation practices consume at least 80% of the available water supply. As a result, precipitation is a key variable affecting public health and political stability (De'Donato and Michelozzi, 2014; Rubio, 2009). One example of this is that drought conditions have been associated with devastating fire seasons across the region, resulting in the destruction of hundreds of hectares of forests and crops even in the relatively more humid and colder regions of the

¹The University of Arizona, USA

²Woods Hole Oceanographic Institution, USA

³Siberian Federal University, Russia

⁴Kahramanmaraş Sütcü İmam Üniversitesi, Turkey

⁵University of Balamand, Lebanon

⁶Forestry Institute, Turkey

⁷Lebanese University, Lebanon

⁸Global Fire Monitoring Center, Germany

⁹Department of Forests, Cyprus

Corresponding author:

Ramzi Touchan, The University of Arizona, Tucson, AZ 85721, USA.
Email: rtouchan@ltrr.arizona.edu

Mediterranean Basin (e.g. Dimitrakopoulos et al., 2011; Pausas et al., 2008). Drought also has profound implications for regional food security, societal upheaval, and economic stability (Kaniewski et al., 2012; Sowers et al., 2011). Quantifying and understanding climatic changes at these regional scales are among the most important and uncertain issues in the study of global change. For example, extreme regional-scale droughts exhibit much larger amplitudes than global averages, and affect regional societies, economies, water supplies, and agricultural ecosystems (e.g. Luterbacher et al., 2004; Xoplaki et al., 2005). Consequently, understanding the spatiotemporal details of drought is of critical importance in this region, where even currently, the consequences can be severe, and an increased occurrence of such events is projected.

Refined knowledge and improved understanding of the full range of past hydroclimatic variability in the EMNE is critical for identifying possible causative factors, evaluating the potential for spatially extensive and temporally persistent anomalies, and for assessing the ability of general circulation models (GCMs) to reproduce variability at timescales from decades to centuries. Meteorological data are sparse in the EMNE and are typically not long enough to effectively capture the potential range of multi-decadal to century-scale variability and the spatiotemporal response to radiative forcing. In view of existing uncertainties, longer records of natural hydroclimatology are necessary for assessing the causes of variability and trends in the instrumental record and evaluating the accuracy of the forced response in forecast GCMs. Touchan et al. (1999, 2003, 2005a, 2005b, 2007, 2008a, 2008b, 2011, 2012), Akkemik and Aras (2005), Akkemik et al. (2008), Köse et al. (2011), Griggs et al. (2007), Hughes et al. (2001), and D'Arrigo and Cullen (2001) have demonstrated that paleoclimate proxy records developed from trees in this region offer a longer term perspective on episodic drought in the EMNE and have identified the steps needed to improve the development and applicability of such records.

In this paper, a network of tree-ring chronologies in the EMNE (33°N–42°N, 21°E–43°E) is described and is analyzed to identify their seasonal climatic signal. This analysis is a preliminary but necessary step toward application of this network to the study of long-term climate variability, the association between regional climate and atmosphere–ocean circulations, and the ability of GCMs to reproduce important drought-related features of regional climate. We apply correlation and cluster analyses to tree-ring and gridded climate data in order to assess the climate signal embedded in the network as preparation for climate field reconstructions and formal proxy/model intercomparison experiments. The objective of the analysis is the improvement and refinement of reconstruction protocols, including the selection of appropriate target reconstruction and climate model fields, all with the larger goal of understanding Mediterranean climate variability at interannual to centennial scales, providing out-of-sample assessment of GCMs, and evaluating the myriad interacting influences on EMNE drought. These analyses also provide complementary data about the variability of climate controls on tree growth across the region that may be useful for predicting the future spatiotemporal response of key forest species to climate change.

Materials and methods

Tree-ring data and chronology development

This study represents the first large-scale systematic dendroclimatic sampling campaign focused on developing a network of drought-sensitive chronologies from Turkey, Syria, Lebanon, Cyprus, and Greece. Fieldwork conducted over the period 2000–2011 has resulted in development of 79 chronologies from 82 tree-ring sites (Table 1 and Figure 1). Samples were collected from species known to form annual rings and those that

demonstrated a high degree of common variation driven by strong climate. Increment cores were taken at all sites, and full cross sections were taken from stumps of cedar and juniper. Samples were surfaced and cross-dated following standard dendrochronological techniques (Stokes and Smiley, 1996). The width of each annual ring on the cores and cross sections was measured to the nearest 0.01 mm.

For the purposes of this study, each series of tree-ring width measurements was fit with a 67% cubic smoothing spline (frequency response 0.50 at a wavelength 2/3 the sample length), to remove nonclimatic trends due to age, size, and the effects of stand dynamics (Cook and Kairiukstis, 1990). The detrended series were then prewhitened with low-order autoregressive models to remove persistence not related to climatic variations. The individual indices were combined into single averaged chronologies for each combination of site and species using a bi-weight robust estimate of the mean (Cook, 1985). Geographic location, confirmed by visual cross-dating and computer-based quality control suggested a strong similarity among several of the resulting 82 residual chronologies. Accordingly, prior to correlation and correlation analysis, the following sites were combined to form single chronologies: (1) PIBR Forest-SYR combines Atera (ATEP), Bait Hamik (BAIP), and Mafrak Bait Ablak (MBAP) and (2) ABCE Forest-SYR combines Bedayat Al Khandak (BKTA) and Rawisat Almedeki (RWIA).

We used expressed population signal (EPS), calculated from data on sample size and between-tree correlation, to assess the adequacy of replication of the chronology (Wigley et al., 1984). The EPS estimates the ability of a finite sample to approximate the true, unknown, population tree-ring signal at the site. Following recommended guidelines (Cook and Kairiukstis, 1990; Wigley et al., 1984), we judged chronologies as adequately sampled for use in climatic reconstruction (e.g. precipitation and drought index) only if the chronology EPS reaches 0.85 before the start of the instrumental climate record.

Climate data and cluster analysis

This analysis was done using 77 of the 79 residual chronologies. We excluded from the analysis two chronologies from Lebanon (HAD, *Cedrus libani*, and KFR, *Pinus pinea*; see Table 2) as they did not cover the full span of the instrumental data (beginning only in 1919 and 1923, respectively). The remaining 77 sites were compared against local monthly gridded climate data. We used 1.0° gridded monthly precipitation data from the Global Precipitation Climatology Centre (GPCC; version 6) dataset covering 1901 through 2010 (Becker et al., 2013; Schneider et al., 2011, 2013) and 0.5° gridded temperature data from the Climatic Research Unit (CRU) TS3.1 dataset (Mitchell and Jones, 2005) covering the period from 1901 to 2009. We also examined the correlation between sites in our network and the Palmer Drought Severity Index (PDSI; Palmer, 1965) developed by Van der Schrier et al. (2013), which covers the period from 1901 to 2009.

We conducted a site-by-site correlation analysis of each residual ring-width chronology against the local (nearest) gridded climate data using the seasonal correlation (Seascorr) procedure developed by Meko et al. (2011) with exact simulation (Percival and Constantine, 2006) for significance testing. We used individual monthly as well as seasonal values integrating 2, 3, or 4 months. We considered a 14-month window starting in the August prior to the growth year and ending in the following September. We then performed a k-means cluster analysis on the resulting 112 monthly and seasonal correlation and partial coefficients for precipitation and temperature for each site. This allows us to analyze groups of chronologies based on their association with their local climate. We estimated the optimal number of clusters using silhouette plots and the gap statistic (Kaufman and Rousseeuw, 1990; Tibshirani et al., 2001).

Table 1. Site information for the eastern Mediterranean region.

Country	Site name	Site code	Latitude (°)	Longitude (°)	Elevation (m)	Species ^a	Time span (year)	Total no. of years	No. of trees/cores
Turkey	Sunanin Barakasi	SUBP	41.35	33.27	1360	1	1682–2009	328	20/40
	Guzelyurt	GUZ	41.05	32.33	1220	1	1585–2009	425	20/40
	Dipsiz Gol	PIG	41.02	33.87	1470	1	1484–2009	526	25/50
	Alaçam Mevkii	ALM	41.00	33.85	1850	1	1709–2009	301	22/44
	Yatak Çamı	YATS	40.82	42.43	2240	2	1757–2001	245	17/34
	Eşek Meydanı	ESE	40.77	42.38	2340	2	1613–2001	389	40/72
	Gavraz	GAV	40.67	36.95	1850	2	1788–2001	214	14/20
	Ayazoğlu Mevkii	AYA	40.62	42.50	2400	1	1770–2001	232	20/37
	Alaçam Deresi	ALD	40.48	31.60	1390	1	1592–2009	418	19/33
	Deliyar	DEL	40.40	32.00	1370	1	1551–2009	459	20/40
	İstasyon Mevkii	IST	40.35	42.55	2400	2	1748–2001	254	19/33
	Tozlu Tepe	TOZ	40.30	39.27	2160	2	1732–2001	270	15/30
	Akyol Deresi	AKY	40.27	42.73	2500	2	1719–2002	284	38/69
	Çal Dağı	CAL	40.23	39.08	1670	2	1787–2001	215	16/30
	Dedeler Mevki	DEM	40.05	26.78	350	1	1715–2010	296	21/40
	Karaören Yaylası	KAY	39.95	31.10	1540	1	1602–2009	408	20/40
	Kavakdağı	KAV	39.60	26.28	510	1	1735–2010	276	20/40
	Uçak Düştü Tepe	UDT	39.41	27.18	830	1	1856–2010	155	20/40
	Kocadağ	KOC	39.41	27.18	1220	1	1823–2010	188	20/40
	Kirazlı	KIR	39.33	29.08	1650	1	1796–2002	207	20/34
	Alıgalani	ALI	39.27	28.85	1650	1	1771–2002	232	23 Dec
	Atalani	ATA	39.23	28.78	1470	1	1792–2002	212	19 Oct
	Dededag	DED	38.53	27.46	1230	1	1698–2010	313	25/50
	Kirikkilise Ziyaret	KIZ	38.00	36.35	1890	1	1776–2009	234	20/40
	Degirmenyüzü	DEY	37.97	36.33	1670	1	1797–2009	213	21/42
	Gokteppe	GOK	37.78	28.95	1400	1	1873–2011	139	20/40
	Honaz Dağı	HOD	37.67	29.26	1660	1	1695–2010	316	26/51
	Circirtepe	CIRP	37.63	35.43	1530	1	1475–2001	527	18/18
	Su Batan	SUBJ	37.42	30.30	1860	3	1246–2000	755	25/36
	Aziziye	AZY	37.42	30.28	1630	1	1511–2001	491	23/35
	Dumanlı Dag	DUD	37.40	30.63	1200	4	1694–2001	218	21/27
	Katrandagi	KATC	37.38	30.60	1470	5	1693–2001	309	23/36
	Karakapi	KAR	37.37	34.58	2030	1	1620–2011	392	21/42
	Şenyayla	SEN	37.31	28.47	1370	1	1590–2010	421	27/52
	Anaardıç	ANA	37.27	34.55	1810	3	1330–2001	672	18/23
	Silpişli	SILJ	37.27	34.55	1790	3	1350–2001	652	17/22
	Üçkuyular	UCK	37.26	29.03	1410	1	1529–2010	482	20/40
	Bozdağ	BOZC	37.26	29.04	1500	5	1770–2010	243	20/40
	Bozdağ	BOZP	37.26	29.04	1510	1	1720–2011	292	20/40
	Bölükandiz	BOLC	37.25	29.07	1850	5	1455–2010	556	38/66
	Neşeli	NESJ	37.20	34.47	1720	3	1235–2011	777	46/73
	Göller	GOLP	37.15	30.52	1050	4	1695–2001	308	22/35
Kartal Gölü	KAG	37.11	28.85	1800	1	1099–2010	912	27/52	
Göller	GOLJ	37.08	30.52	1050	3	1152–2000	849	22/40	
Bayat Bademleri	BAB	37.03	30.47	700	4	1738–2001	264	15/15	
Arpa Alani	ARAJ	36.95	34.08	1980	3	1121–2001	874	27/33	
Kozlu Pinari	KOP	36.65	32.20	1640	1	1586–2000	415	16/24	
Yellic Beli	YEB	36.65	32.18	1730	5	1628–2000	373	16/24	
Elmalı	ELMJ	36.60	30.02	1950	3	1017–2006	990	51/108	
Elmalı	ELMC	36.60	30.02	1950	5	1449–2001	553	50/70	
Greece	Mount. Olympus	MOL	40.08	22.37	2130	6	1506–2010	505	37/67
	Valia Kalda	VKA	39.92	21.13	1550	1	1196–2010	815	68/140
	Pefkas	PEF	37.96	22.40	1590	1	1637–2011	375	29/58
	Kanistro	KAS	37.85	22.36	1370	7	1870–2011	142	25/50
	Potistiria	POT	35.30	23.92	970	4	1842–2009	168	21/42
Cyprus	Anapoli Low	ANAL	35.23	24.07	800	4	1888–2009	122	20/40
	Anapoli High	ANAH	35.23	24.10	1050	4	1879–2009	131	21/42
	Stavrostis Psokas	STP	35.02	32.63	1059	4	1839–2002	263	20/38
	Amforitis	AMF	35.00	32.63	859	4	1714–2010	297	21/42
Cyprus	Tripylos	TRI	34.99	32.68	1352	8	1532–2010	479	20/40
	Amiandos	AMB	34.94	32.92	1489	4	1549–2010	462	36/72
	Amiandos	AMIN	34.94	32.90	1640	1	1554–2002	449	20/40

(Continued)

Table 1. (Continued)

Country	Site name	Site code	Latitude (°)	Longitude (°)	Elevation (m)	Species ^a	Time span (year)	Total no. of years	No. of trees/cores
Syria	Chionistra	CHI	34.94	32.87	1776	1	1379–2002	624	22/44
	Turpland	TUL	34.93	32.90	1642	1	1435–2010	576	20/40
	Artemio	ART	34.93	32.87	1815	1	1410–2010	601	20/40
	Hatzipaylou Mine	HAM	34.92	32.86	1756	1	1288–2010	723	20/40
	Atera	ATEP	35.83	36.02	440	1	1892–2001	110	7 Jul
	Bait Hamik	BAIP	35.78	35.98	510	4	1882–2001	120	21/25
	Mafrak Bait Ablak	MBAP	35.78	36.02	560	4	1901–2001	101	11 Oct
	Kumat Bani Mata	KNM	35.60	36.22	1450	5	1837–2001	165	19/20
	Bedayat Al Khandak Al Tawil	BKTA	35.57	36.20	1410	9	1830–2001	172	16/17
	Rawisat Almedeki	RWIA	35.55	36.20	1480	9	1795–2001	207	17/18
Lebanon	Kamouaa	KAM	34.48	36.23	1559	5	1808–2009	202	20/40
	Wadi El Blat	WAB	34.47	36.23	1170	9	1722–2001	280	16/19
	Jurd Al Njas	JRA	34.39	36.18	1810	5	1852–2010	159	17/34
	Ehden Reserve	EHD	34.31	35.99	1640	5	1792–2010	219	33/45
	Hadath	HAD	34.24	35.92	1500	5	1918–2011	94	20/40
	Bsharri	BSH	34.24	36.05	1940	5	1374–2010	637	53/109
	Kfloor El Aarbeh	KFR	34.22	35.86	980	10	1921–2011	91	20/40
	Tannourine	TAN	34.21	35.93	1760	5	1801–2011	211	31/59
	Arz Jaj	ARJ	34.15	35.82	1670	5	1778–2011	234	56/88
	Maaser Al Shouf	MAA	33.69	35.69	1700	5	1730–2010	281	33/62

^aSpecies key: 1. *Pinus nigra*, 2. *Pinus sylvestris*, 3. *Juniperus excelsa*, 4. *Pinus brutia*, 5. *Cedrus libani*, 6. *Pinus heldreichii*, 7. *Abies cephalonica*, 8. *Cedrus brevifolia*, 9. *Abies cilicica* and 10. *Pinus pinea*.

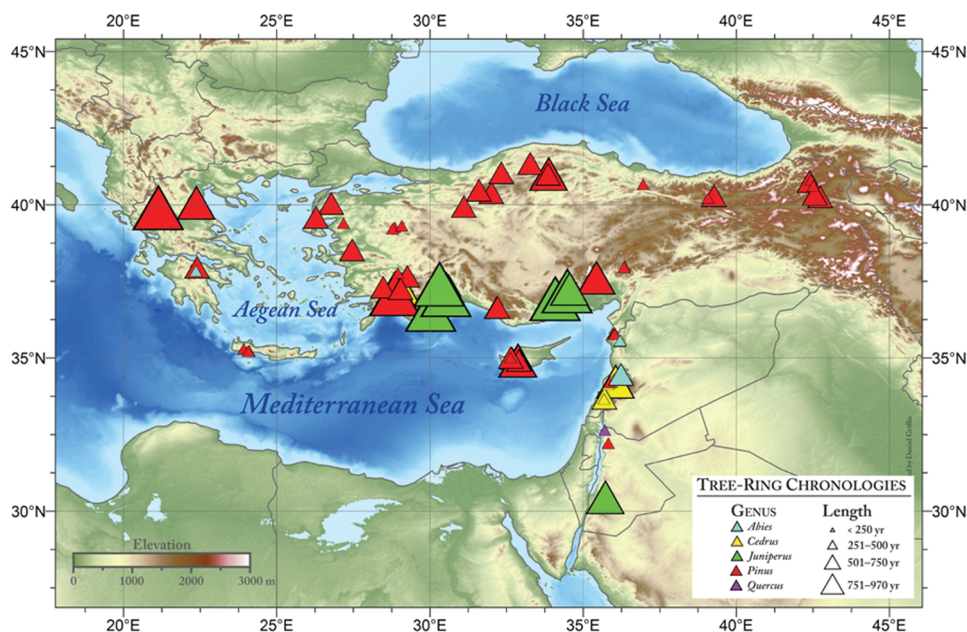


Figure 1. Locations of tree-ring chronology sites, with symbol color and size indicating genus and length, respectively.

Results

Tree-ring chronologies

Data for individual tree-ring chronologies are summarized in Tables 1 and 2. The lengths of the 79 chronologies range from 89 (Hadath, Lebanon) to 990 years (Elmali, Turkey; Table 1). Statistical analyses of each chronology are summarized in Table 2. The mean correlation among individual radii at each site (the interseries correlation) represents the strength of their common signal and ranges from 0.17 to 0.59. The highest interseries correlation is for the NESJ site in Turkey, and the lowest is for the chronology developed from the JRA site in Lebanon. The EPS of three chronologies (including the two already eliminated from consideration

due to their limited time span) fails to reach 0.85 by the start of the climatic record, leaving a total of 76 chronologies potentially useful for climatic reconstruction without additional sampling. The mean sample segment length (MSSL) of all 79 chronologies ranges from 68 to 408 years. Half of these chronologies have a MSSL greater than 200 years in length, and several have MSSL exceeding 400 years.

Climate and cluster analysis

Analysis of monthly correlations and partial correlations between gridded climate data and our tree-ring width chronologies reveals a pervasive positive association with May, June,

Table 2. Summary statistics for the 79 chronologies for the ARSTAN program (Cook and Holmes, 1999; Cook and Krusic, 2005).

Country	Site code	Total chronology				Common interval			
		MSSL	Std	SK	KU	1st year EPS > 0.85	Time span	MCAR	EV PCI (%)
Greece	MOL	203	0.15	-0.13	0.53	1613	1890–2008	0.35	37
	VKA	355	0.20	0.22	0.39	1279	1709–1992	0.38	40
	PEF	217	0.15	-0.99	5.98	1687	1873–2008	0.35	37
	KAS	112	0.15	-0.07	-0.36	1885	1924–2007	0.42	45
	POT	97	0.20	0.21	0.83	1909	1932–2008	0.41	44
	ANAL	70	0.23	0.09	0.43	1921	1962–2008	0.52	55
	ANAH	87	0.22	0.21	2.62	1910	1939–2004	0.45	47
Turkey	SUBP	235	0.18	0.25	0.57	1728	1792–2000	0.40	42
	GUZ	235	0.19	0.35	0.97	1781	1807–2004	0.38	40
	PIG	263	0.19	-0.22	0.67	1709	1772–2008	0.37	40
	ALM	233	0.13	0.70	3.80	1770	1822–1996	0.31	34
	YATS	186	0.13	0.21	0.79	1803	1853–2001	0.32	35
	ESE	239	0.14	0.48	1.07	1682	1837–2001	0.34	36
	GAV	170	0.16	0.22	0.10	1804	1812–2001	0.48	49
	AYA	175	0.12	0.02	0.19	1802	1857–2001	0.33	35
	ALD	248	0.24	0.66	1.25	1700	1850–2009	0.43	45
	DEL	207	0.20	0.09	0.28	1757	1828–1999	0.43	46
	IST	144	0.11	-0.13	0.57	1846	1905–2001	0.26	29
	TOZ	166	0.15	0.65	0.55	1799	1885–2000	0.47	50
	AKY	200	0.12	-0.07	1.00	1757	1855–2001	0.35	35
	CAL	150	0.17	0.28	1.18	1836	1890–1997	0.32	35
	DEM	167	0.24	0.51	1.44	1866	1894–2010	0.32	35
	KAY	212	0.17	-0.13	0.35	1775	1830–2009	0.37	40
	KAV	185	0.22	-0.04	0.75	1806	1871–2010	0.36	38
	UDT	108	0.15	0.46	0.46	1910	1925–2007	0.27	30
	KOC	139	0.17	0.37	0.73	1883	1895–2012	0.28	31
	KIR	175	0.20	0.70	1.99	1823	1851–2002	0.49	50
	ALI	162	0.19	0.06	-0.11	1850	1861–2001	0.40	45
	ATA	190	0.18	0.17	-0.04	1809	1844–2001	0.41	45
	DED	238	0.11	0.24	0.30	1789	1836–2010	0.24	27
	KIZ	245	0.20	0.37	0.19	1727	1779–2010	0.39	41
	DEY	154	0.14	-0.45	1.55	1844	1880–2009	0.35	37
	GOK	107	0.16	0.19	0.58	1898	1912–2011	0.36	39
	HOD	169	0.15	0.06	0.38	1863	1883–2010	0.28	31
	CIRP	390	0.20	0.40	3.82	1577	1689–2001	0.37	41
	SUBJ	299	0.18	0.12	0.14	1338	1672–1950	0.44	50
	AZY	204	0.13	0.08	0.00	1789	1861–2000	0.31	34
	DUD	146	0.20	0.23	0.53	1831	1893–1999	0.48	51
	KATC	157	0.18	0.17	0.20	1815	1878–2000	0.47	49
	KAR	238	0.11	0.24	0.30	1789	1836–2010	0.24	27
	SEN	245	0.20	0.37	0.19	1727	1779–2010	0.39	41
	ANA	231	0.17	0.38	0.18	1736	1797–2001	0.40	46
	SILJ	218	0.22	0.24	0.14	1727	1890–2000	0.52	56
	UCK	183	0.18	0.29	0.39	1741	1845–2010	0.49	53
	BOZC	91	0.20	0.01	1.08	1940	1959–2011	0.36	39
	BOZP	172	0.21	0.27	0.27	1811	1872–2009	0.46	48
	BOLC	206	0.22	0.10	1.24	1523	1851–2010	0.48	50
	NESJ	408	0.25	0.12	-0.01	1296	1579–1976	0.59	60
	GOLP	169	0.17	0.32	0.94	1798	1885–1999	0.48	50
KAG	367	0.13	0.12	0.30	1557	1582–2010	0.26	31	
GOLJ	341	0.16	0.14	0.49	1594	1759–2000	0.32	36	
BAB	171	0.19	-0.50	0.25	1751	1797–1996	0.59	65	
ARAJ	357	0.18	0.70	2.02	1616	1719–1976	0.33	37	
KOP	295	0.15	0.24	0.91	1682	1744–2000	0.31	35	
YEB	200	0.19	0.18	0.26	1743	1818–2000	0.36	41	
ELMJ	316	0.20	0.41	0.17	1102	1703–1960	0.42	44	
ELMC	330	0.17	-0.40	1.21	1505	1759–1997	0.48	50	
Cyprus	STP	213	0.16	-0.02	1.15	1765	1829–2002	0.37	39
	AMF	169	0.16	-0.03	0.64	1779	1844–2010	0.37	40
	TRI	241	0.19	0.66	2.71	1719	1813–2002	0.37	38
	AMB	200	0.17	0.34	1.08	1734	1842–2002	0.40	42
	AMIN	325	0.14	0.16	0.61	1591	1640–1934	0.30	33
	CHI	332	0.19	0.62	0.81	1596	1727–2002	0.41	44

(Continued)

Table 2. (Continued)

Country	Site code	Total chronology				Common interval			
		MSSL	Std	SK	KU	1st year EPS > 0.85	Time span	MCAR	EV PCI (%)
Syria	TUL	315	0.18	0.52	2.76	1605	1788–2010	0.40	42
	ART	332	0.18	0.41	0.16	1719	1731–1998	0.37	40
	HAM	275	0.21	0.07	5.26	1629	1786–2005	0.46	48
	PIBR ¹	89	0.13	-0.39	0.08	1909	1937–2000	0.20	24
	KNM	99	0.20	0.16	0.04	1883	1921–2001	0.36	41
	ABCE ²	110	0.25	0.77	2.86	1872	1913–2000	0.26	31
Lebanon	KAM	120	0.20	0.40	2.67	*	1921–2009	0.20	23
	WAB	137	0.14	-0.22	0.44	1876	1913–2001	0.22	28
	JRA	86	0.13	0.14	0.93	*	1928–2009	0.17	24
	EHD	128	0.13	-0.29	0.55	1866	1891–2001	0.37	40
	HAD	75	0.09	0.15	0.66	*	1950–2011	0.20	24
	BSH	278	0.19	-0.32	0.93	1547	1807–1993	0.42	44
	KFR	68	0.15	0.80	1.26	1949	1959–2011	0.26	29
	TAN	128	0.19	-0.01	0.15	1857	1910–2010	0.41	44
	ARJ	113	0.14	0.10	0.48	1875	1925–2001	0.31	34
	MAA	151	0.19	-0.40	0.90	1757	1881–2002	0.44	46

MSSL: mean sample segment length; Std: standard deviation; SK: skewness; KU: Kurtosis; EPS: Expressed Population Statistic (Wigley et al., 1984); MCAR: mean correlation among radii; EV: explained variance.

¹Brutia pine forest combines ATER, BAIP, and MBAP.

²*Abies cilicica* forest combines BKTA and RWIA.

*More samples are needed.

and sometimes July precipitation; positive correlations with winter and spring (December through April) temperatures; and negative relationships with May through July temperature, although as expected, there are site-to-site exceptions to these general patterns (Figure 2).

Our cluster analysis suggests three groups of sites based on their association with climate. Iterative testing of the gap statistic (Tibshirani et al., 2001) suggests that the data could reasonably be represented by 2, 3, or 5 clusters. Using only two clusters, however, failed to fully capture differences in the climate response seen in Figure 2, while analyses using five clusters resulted in the apparently spurious development of small clusters consisting of only one or two sites and whose climate response could not be differentiated from other clusters. Therefore, we proceed with our analysis for the results using three clusters.

The average climate response of the three clusters is shown in Figures 3–5. These indicate (1) a cluster characterized by a May–June positive precipitation response and a positive seasonal temperature response throughout most of the late prior and current growing season, (2) a cluster with a positive precipitation response in May–June with a negative temperature response during the summer and a negligible temperature response during the spring and winter, and (3) a cluster with a positive May–June precipitation response, a positive winter–spring temperature response, and a subsequent and abrupt negative temperature response during summer.

A map of the distribution of the site cluster assignments (Figure 6) shows that Clusters 2 and 3 are intermingled across the domain, although Cluster 2 contains fewer sites (24, compared with 38 in Cluster 3), is broadly coastal, and is predominantly located in the Levant and Greece. Cluster 3 is the largest and is composed of the majority of the sites throughout Turkey, Cyprus, and Crete. The majority of the sites within Cluster 1 are found in northeastern Turkey.

We can examine the distribution of species across our cluster (Figure 7). Cluster 1 contains all the *Pinus sylvestris* (PISY) sites, but also one *Pinus nigra* (PINI) chronology, several *Juniperus*

excelsa (JUEX) sites, and a *C. libani* (CDLI) chronology. Cluster 1 sites are also encountered at significantly higher elevations than Cluster 2 or 3 (Figure 8). For Clusters 2 and 3, the remaining *P. nigra* and *J. excelsa* chronologies are distributed between them. The majority of the *C. libani* chronologies are in Cluster 2 as are all the *Abies* sites, while Cluster 3 contains all the *Pinus brutia* (PIBR) chronologies and the *Cedrus brevifolia* (CDBR) site.

The observed positive correlations with summer precipitation and negative correlations with coeval temperatures suggest that integrated measures of water availability could represent an even stronger control on tree growth at some sites in our network. Figure 9 shows the correlation between the chronologies in our network and the local PDSI from Van der Schrier et al. (2013). PDSI incorporates the influence of precipitation, evaporation, and storage into a metric of water balance. Correlations with spring–summer (May through August) or summer (June through August) PDSI in our network are positive over the region, with the strongest correlations seen in western and northern Turkey.

Discussion

The chronology statistics and cluster analysis attest to the potential value of this 79-chronology tree-ring network for climate reconstruction. Replication and time span are currently sufficient at 76 sites for the chronologies to characterize the common tree-growth signal at the site. More samples could also render the remaining three sites, all in Lebanon (KAM, JRA, and HAD), useful for climate reconstructions.

One of the major objectives of dendroclimatology is to obtain the longest possible tree-ring records from living and dead trees to investigate climate variability over several centuries or longer. Throughout most of the eastern Mediterranean, we have been able to collect samples that were several hundred years in age. This has been accomplished primarily by applying knowledge originally developed over many decades in the semi-arid North American southwest region in the selection of species (distinct annual rings), sites (a single climatic factor limiting to growth), and

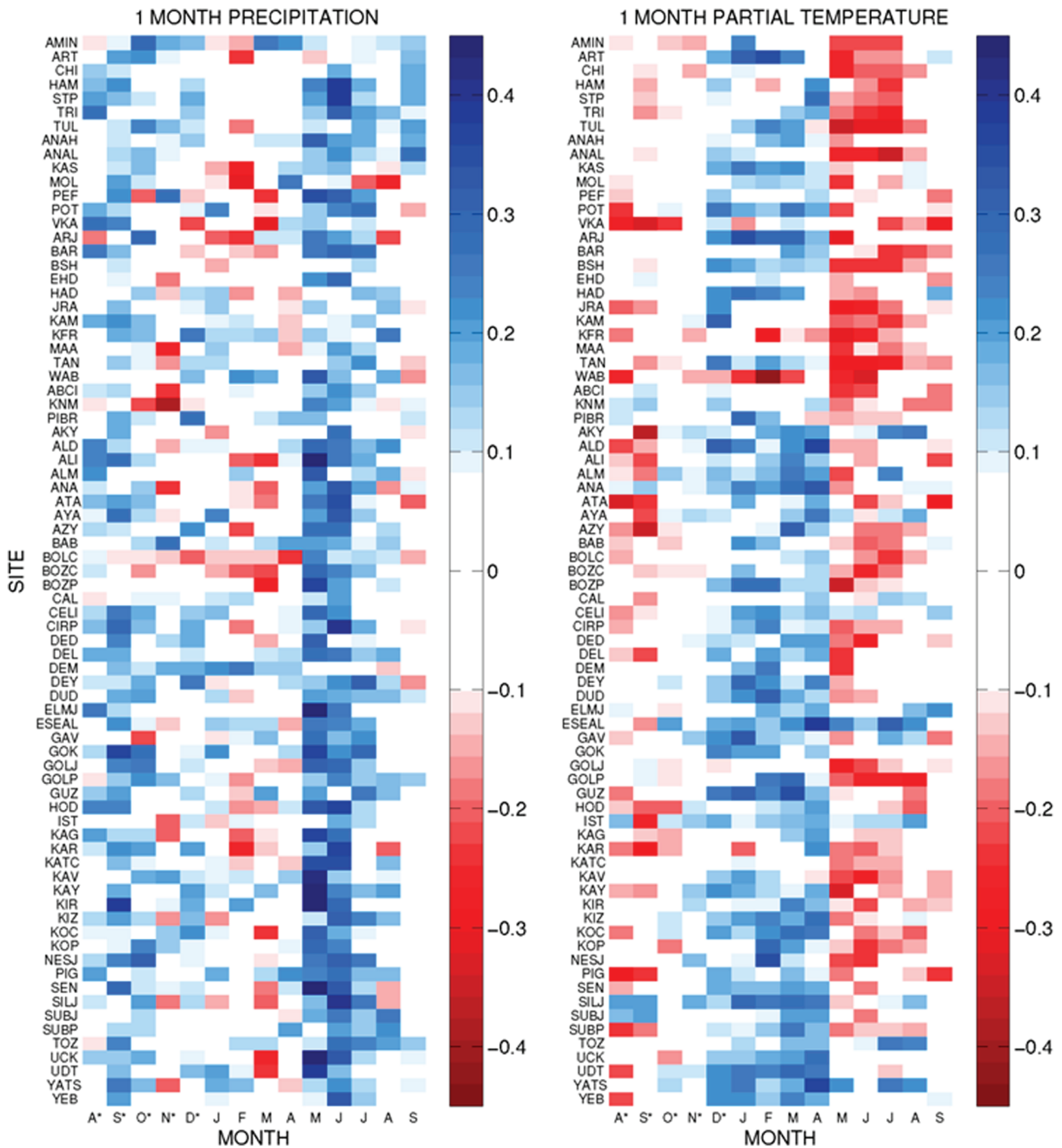


Figure 2. Monthly correlations with total GPCP v6 1 precipitation (Becker et al., 2013; Schneider et al., 2013) for each eastern Mediterranean site used in the network analysis and partial correlations with mean CRU TS3.1 0.5 temperature (Mitchell and Jones, 2005) for each eastern Mediterranean site used in the network analysis. Sites are correlated against the closest grid cell in each dataset. GPCP: Global Precipitation Climatology Centre; CRU: Climatic Research Unit.

individual trees (many rings and large year-to-year variability in ring width) for analysis (e.g. Fritts, 1976). Furthermore, multi-century mean segment lengths ensure that series span sufficient time to be adequate for the investigation of multidecadal and centennial climate variability when combined with conservative detrending and standardization (Cook et al., 1995).

Some elevational dependence is evident in the clusters. Sites in Cluster 1 are at a significantly higher elevation (Figure 8; cf. McGill et al., 1978), consistent with the location of the *P. sylvestris* that comprise this cluster, while Clusters 2 and 3 are composed of sites at lower elevations but are not distinguishable from one another. The dependence on elevation may reflect a tendency for the species themselves to be stratified by elevation or could

also suggest climate regimes determined by topography or elevation (e.g. high mountain) that can impose similar tree-growth variations in chronologies from widely separate locations (Bhattarai and Vetaas, 2006; Lenoir et al., 2008).

Although individual sites can reflect a diversity of monthly or seasonal climate responses, considered across the entire network of 76 sites, a number of consistent features emerge from our cluster analysis: most of the network has an early summer (May–June) positive response to precipitation. Similar results have been reported by Touchan et al. (2003, 2007), Griggs et al. (2007), Akkemik et al. (2008), and Köse et al. (2011), who likewise investigated the relationship between climate and tree-ring data in the region. Hughes et al. (2001) evaluated specimens from living

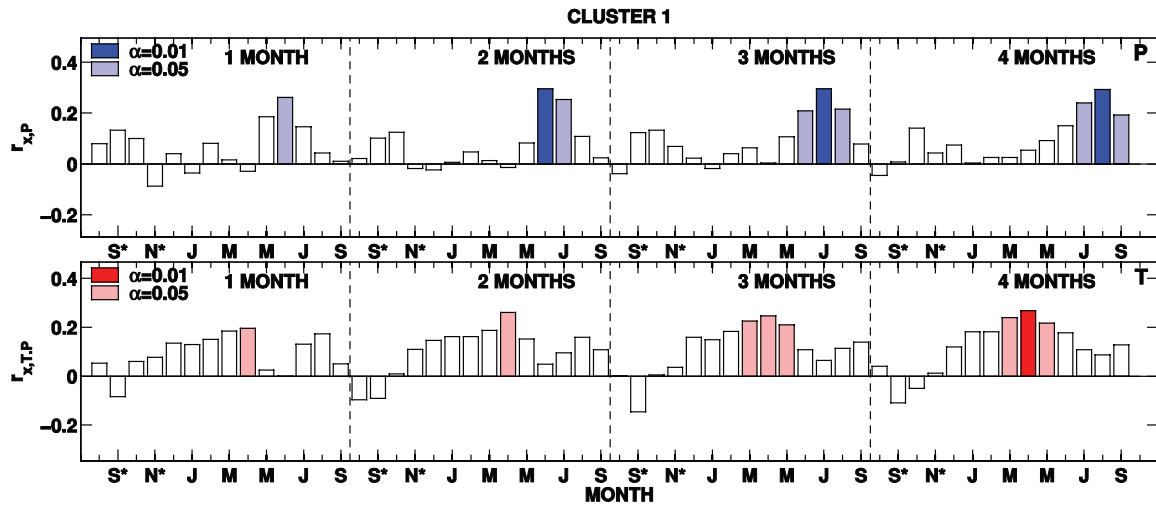


Figure 3. Median monthly and seasonal correlation and partial correlation response from SEASCORR of the tree-ring chronologies belonging to Cluster 1. Significance levels shown here are the median of those determined by exact simulation (Meko et al., 2011; Percival and Constantine, 2006) for each individual site.

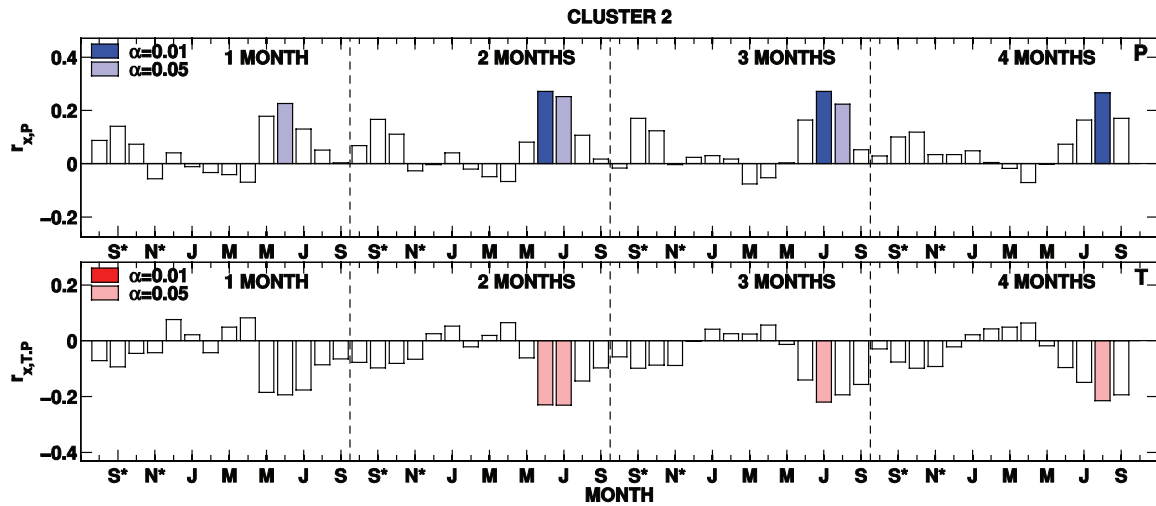


Figure 4. Median monthly and seasonal correlation and partial correlation response from SEASCORR of the tree-ring chronologies belonging to Cluster 2. Significance levels shown here are the median of those determined by exact simulation (Meko et al., 2011; Percival and Constantine, 2006) for each individual site.

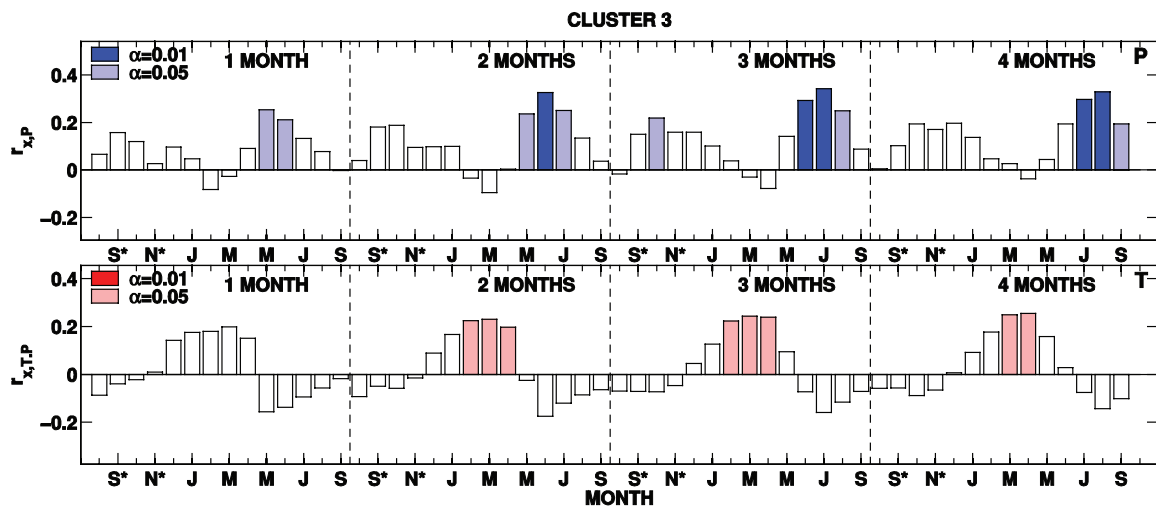


Figure 5. Median monthly and seasonal correlation and partial correlation response from SEASCORR of the tree-ring chronologies belonging to Cluster 3. Significance levels shown here are the median of those determined by exact simulation (Meko et al., 2011; Percival and Constantine, 2006) for each individual site.

tree chronologies from southeastern Europe to the eastern Mediterranean. They demonstrated that cross-dating over large distances in Greece and Turkey has a clear climatological basis, with signature years consistently being associated with specific, persistent atmospheric circulation anomalies. They reported that the most consistently significant relationship of tree-ring growth to climate data was the positive growth response to spring and early summer precipitation, particularly April–June in the eastern Mediterranean. Touchan et al. (2003, 2007) found that precipitation in May and/or June is most consistently the controlling factor of tree-ring growth in a regional chronology from southwestern Anatolia in Turkey. Touchan et al. (2005b) conducted the first large-scale

systematic dendroclimatic sampling for this region using a diversity set of species. Their response function analysis identified May–August total precipitation as the most appropriate seasonal predictand for reconstruction based on consistent patterns of monthly series with significant response function elements of the same sign. Akkemik and Aras (2005) reported that oak tree-ring growth is influenced by March–June precipitation in western Black Sea region of Turkey. Griggs et al. (2007) developed a May–June precipitation reconstruction for northeastern Greece and northwestern Turkey. They reported that negative mean temperature of May and June is also a growth-limiting factor owing to its effect on the availability of precipitation to the trees but is more difficult to calibrate and reconstruct accurately owing to the trees’ indirect response and the low number of long temperature records available for the interior of northwestern Turkey. Köse et al. (2011) conducted a dendroclimatic study of 17 black pine (*P. nigra*) chronologies in western Anatolia, Turkey, and reported that the influence of precipitation on tree-ring growth was positive and significant in May in almost all regions. A positive but less significant influence was found for June. Their results revealed that the most important factor affecting tree-ring width of black pine was May–June precipitation in western Anatolia.

Temperature responses across our sites are more diverse than those with precipitation but generally fall into one of the three categories: a positive response to winter–spring temperature, a positive response to response in nearly all seasons, and a negative response to temperature during the summer. The clearest difference among the clusters we have identified here is between Cluster 1, characterized by higher elevation *P. sylvestris* in northeastern Turkey with a positive temperature response through most of the year, and lower elevation sites throughout Turkey, Greece, and the Levant in Clusters 2 and 3 with May–June precipitation responses

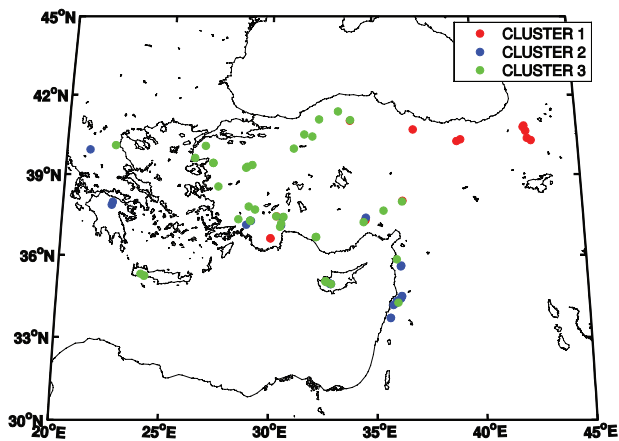


Figure 6. Cluster assignment for sites in the eastern Mediterranean tree-ring chronology network.

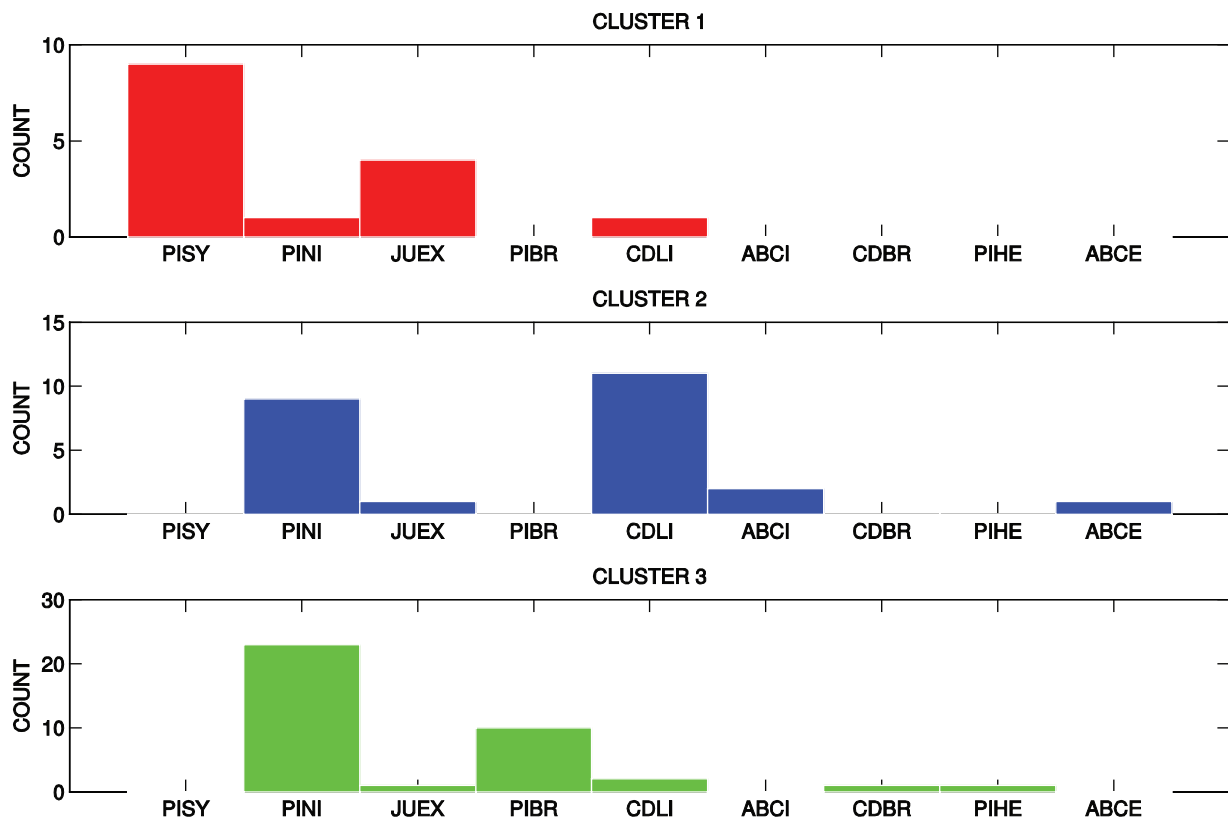


Figure 7. Cluster assignment for species in the eastern Mediterranean tree-ring chronology network. International Tree-Ring Data Bank species codes are *Pinus sylvestris* (PISY), *Pinus nigra* (PINI), *Juniperus excelsa* (JUEX), *Pinus brutia* (PIBR), *Cedrus libani* (CDLI), *Abies cilicica* (ABCI), *Cedrus brevifolia* (CDBR), *Pinus heldreichii* (PIHE), and *Abies cephalonica* (ABCE). Species collected during sampling and not part of the 77 chronologies analyzed here are not shown.

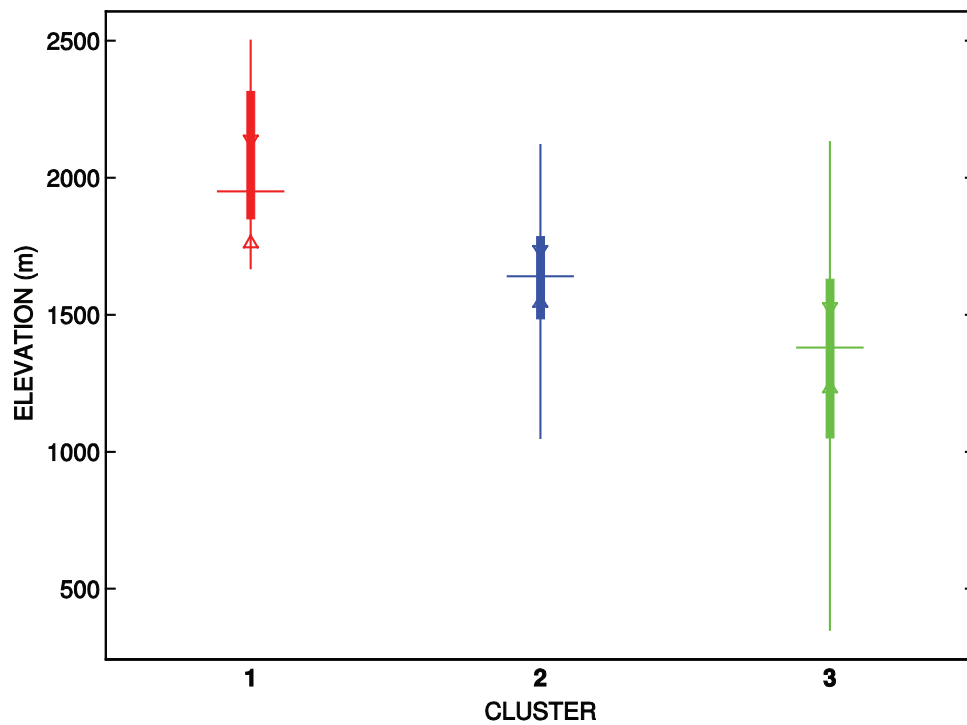


Figure 8. Boxplots showing elevation for chronologies within each cluster. Horizontal lines through each box indicate the median value. The edges of the box indicate the 25th and 75th percentiles, and the whiskers reflect the full range of the site elevation in each cluster. Triangles indicate the comparison intervals for the median (McGill et al., 1978), indicating Cluster 1 is significantly different from Clusters 2 and 3.

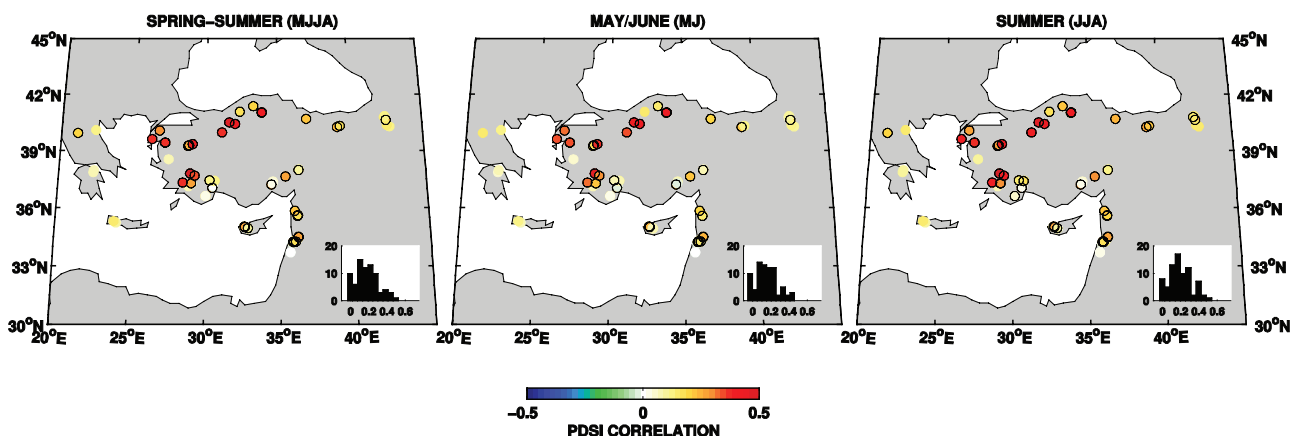


Figure 9. Correlations between tree-ring chronologies and the corresponding local gridded PDSI from Van der Schrier et al. (2013) over their respective common intervals. Colors indicate Pearson product-moment correlation coefficients and those sites where $p < 0.10$ have an additional black outline. Inset histograms show the frequency (y-axis) of correlation coefficients (x-axis). Panels correspond to the mean May-through-August PDSI (left), mean May and June PDSI (center), and mean June through August PDSI (right).

dominated by *P. nigra*. Cluster 2 tends to be found near the Mediterranean and has no positive response to temperature, while Cluster 3 is widespread throughout Anatolia and switches from a positive response to winter–spring temperature to a negative response during the summer and coincident with a positive correlation with precipitation.

The PDSI is a common target for paleoclimate field reconstructions (e.g. Cook et al., 1999, 2004, 2010; Touchan et al., 2011) since it is designed to capture the balance between precipitation and evapotranspiration and may therefore be a better indicator of effective moisture conditions than either variable alone. The combination of positive precipitation correlations and negative summer temperature correlations across a swath of our network suggests that the PDSI is a reasonable variable to reconstruct in this region. Positive correlation with spring–summer (May through August) and summer (June through August) PDSIs is

observed across our network (Figure 9). Interestingly, the highest correlations are seen throughout western and northern Turkey, where they largely correspond to the sites in Cluster 3. Sites in Cluster 3 have overall correlations with summer PDSI more than twice those of the other clusters, although even Cluster 1 with its broad positive associations with temperature throughout the year shows positive correlations with PDSI. These observations indicate that, in addition to May–June precipitation, either May–August (MJJA) or June–August (JJA) PDSI is a reasonable target for climate field reconstruction in our region, and that PDSI appears to be strongly controlled by precipitation.

Conclusion

This study represents the first large-scale systematic dendroclimatic sampling focused specifically on developing a network of

tree-ring chronologies from multiple species from Turkey, Greece, Cyprus, Syria, and Lebanon. This network of chronologies contains coherent seasonal precipitation and temperature signals across a fairly broad geographical area, in particular a common significant response to May–June precipitation. Collectively, these findings suggest that it may be possible to reconstruct three fields from these data. May–June precipitation is an important control on nearly the entire network, while the negative association with summer temperatures suggests that the PDSI is an additional and reasonable reconstruction target. Finally, the existence of a winter–spring and even in some cases summer temperature signal, particularly in *P. sylvestris* from northeastern Turkey, suggest the possibility of performing temperature reconstructions over at least part of the eastern Mediterranean domain.

Acknowledgements

We wish to thank the different Forestry Departments in Turkey, Greece, Cyprus, Lebanon, and Syria for their great help and support in making this study possible. We would like to thank Cyprus Meteorological Service for providing us with climate data. We thank Professor Alexandros P Dimitrakopoulos from the Laboratory of Forest Protection, School of Forestry and Natural Environment, Aristotle University of Thessaloniki, Greece, for his help and support. We thank Christopher Baisan, Russell Biggs, and Gurudas C Bock for their valuable assistance in the field. We also thank Russell Biggs, Victoria L Frazier, Alicia Stout, Gurudas C Bock, Jessica L Little, and Anthony P Trujillo for their assistance in sample preparation and measurement. We thank Daniel Griffin for developing Figure 1. We wish to thank the anonymous reviewers for their constructive comments and suggestions on the manuscript.

Funding

Funding was provided by the US National Science Foundation under Grant Earth System History (grant no. 0075956) and ATM-GEO/ATM-Paleoclimate Program 0758486.

References

- Akkemik Ü and Aras A (2005) Reconstruction (1689–1994 AD) of April–August precipitation in the southern part of central Turkey. *International Journal of Climatology* 25: 537–548.
- Akkemik Ü, D'Arrigo R, Cherubini P et al. (2008) Tree-ring reconstructions of precipitation and streamflow for north-western Turkey. *International Journal of Climatology* 28(2): 173–183.
- Alpert P, Osetinsky I, Ziv B et al. (2004) Semi-objective classification for daily synoptic systems: Application to the eastern Mediterranean climate change. *International Journal of Climatology* 24: 1001–1011.
- Bartzokas A, Metaxas DA and Ganas IS (1994) Spatial and temporal sea-surface temperature covariances in the Mediterranean. *International Journal of Climatology* 14: 201–213.
- Becker A, Finger P, Meyer-Christoffer A et al. (2013) A description of the global land-surface precipitation data products of the Global Precipitation Climatology Centre with sample applications including centennial (trend) analysis from 1901 to present. *Earth System Science Data* 5(1): 71–99.
- Bhattarai KR and Vetaas OR (2006) Can Rapoport's rule explain tree species richness along the Himalayan elevation gradient, Nepal? *Diversity and Distributions* 12: 373–378.
- Cook ER (1985) *A time-series analysis approach to tree-ring standardization*. PhD Dissertation, Department of Geosciences, The University of Arizona.
- Cook ER and Holmes RL (1999) *Program ARSTAN – Chronology Development with Statistical Analysis* (user's manual for program ARSTAN). Tucson, AZ: Laboratory of Tree-Ring Research, University of Arizona, 18 pp.
- Cook ER and Kairiukstis L (1990) *Methods of Dendrochronology: Applications in the Environmental Sciences*. Dordrecht: Kluwer Academic Publishers.
- Cook ER and Krusic PJ (2005) *ARSTAN v. 41d: A Tree-Ring Standardization Program Based on Detrending and Autoregressive Time Series Modeling, with Interactive Graphics*. New York: Tree-Ring Laboratory, Lamont-Doherty Earth Observatory, Columbia University. Available at: <http://www.ldeo.columbia.edu/tree-ring-laboratory/resources/software>.
- Cook ER, Anchukaitis KJ, Buckley BM et al. (2010) Asian monsoon failure and megadrought during the last millennium. *Science* 328(5977): 486–489.
- Cook ER, Briffa KR, Meko DM et al. (1995) The segment length curse in long tree-ring chronology development for paleoclimatic studies. *The Holocene* 5: 229–237.
- Cook ER, Meko DM, Stahle DW et al. (1999) Drought reconstructions for the continental United States. *Journal of Climate* 12(4): 1145–1162.
- Cook ER, Woodhouse CA, Eakin CM et al. (2004) Long-term aridity changes in the western United States. *Science* 306(5698): 1015–1018.
- Corte-Real S, Zhang X and Wang X (1995) Large-scale circulation regimes and surface climatic anomalies over the Mediterranean. *International Journal of Climatology* 15: 413–424.
- D'Arrigo RD and Cullen HM (2001) A 350-year (AD 1628–1980) reconstruction of Turkish precipitation. *Dendrochronologia* 19: 169–177.
- De'Donato F and Michelozzi P (2014) Climate change, extreme weather events and health effects. In: Goffredo S and Dubinsky Z (eds) *The Mediterranean Sea*. Dordrecht: Springer, pp. 617–624.
- Dimitrakopoulos AP, Vlahou MA, Anagnostopoulou ChG et al. (2011) Impact of drought on wildland fires in Greece: Implications of climatic change? *Climatic Change* 109: 331–347.
- Duenkeloh A and Jacobeit J (2003) Circulation dynamics of Mediterranean precipitation variability 1948–1998. *International Journal of Climatology* 23: 1843–1866.
- Fritts HC (1976) *Tree Rings and Climate*. London: Academic Press, 576 pp.
- Griggs C, DeGaetano A, Kuniholm P et al. (2007) A regional high-frequency reconstruction of May–June precipitation in the north Aegean from oak tree rings, A.D. 1089–1989. *International Journal of Climatology* 27: 1075–1089.
- Hughes MK, Kuniholm PI, Garfin GM et al. (2001) Aegean tree-ring signature years explained. *Tree-Ring Research* 57(1): 67–73.
- Kaniewski D, Campo EV and Weiss H (2012) Drought is a recurring challenge in the Middle East. *Proceedings of the National Academy of Sciences of the United States of America* 109(10): 3862–3867.
- Kaufman L and Rousseeuw PJ (1990) *Finding Groups in Data: An Introduction to Cluster Analysis*. Hoboken, NJ: John Wiley & Sons, Inc.
- Köse N, Akkemik Ü, Dalfes HN et al. (2011) Tree-ring reconstructions of May–June precipitation for western Anatolia. *Quaternary Research* 75(3): 438–450.
- Lenoir J, Gégout JC, Marquet PA et al. (2008) A significant upward shift in plant species optimum elevation during the 20th century. *Science* 320(5884): 1768–1771.
- Lolis CJ, Bartzokas A and Metaxas DA (1999) Spatial covariability of the climatic parameters in the Greek area. *International Journal of Climatology* 19: 185–196.
- Luterbacher J, Dietrich D, Xoplaki E et al. (2004) European seasonal and annual temperature variability, trends, and extremes since 1500. *Science* 303: 1499–1503.

- McGill R, Tukey JW and Larsen WA (1978) Variations of box plots. *The American Statistician* 32(1): 12–16.
- Mariotti A, Struglia MV, Zeng N et al. (2002) The hydrological cycle in the Mediterranean region and implications for the water budget of the Mediterranean Sea. *Journal of Climate* 15: 1674–1690.
- Meko DM, Touchan R and Anchukaitis KJ (2011) Seascorr: A MATLAB program for identifying the seasonal climate signal in an annual tree-ring time series. *Computers & Geosciences* 37(9): 1234–1241.
- Mitchell T and Jones P (2005) An improved method of constructing a database of monthly climate observations and associated high-resolution grids. *International Journal of Climatology* 25: 693–712.
- Palmer WC (1965) *Meteorological drought*. Research paper no. 45, February, 58 pp. Washington, DC: U.S. Department of Commerce.
- Pausas JG, Llovet J, Rodrigo A et al. (2008) Are wildfires a disaster in the Mediterranean basin? – A review. *International Journal of Wildland Fire* 17: 713–723.
- Percival DB and Constantine WL (2006) Exact simulation of Gaussian time series from nonparametric spectral estimates with application to bootstrapping. *Statistics and Computing* 16(1): 25–35.
- Raicich F, Pinaridi N and Navarra A (2003) Teleconnections between Indian monsoon and Sahel rainfall and the Mediterranean. *International Journal of Climatology* 23: 173–186.
- Rodwell MR and Hoskins BJ (1996) Monsoons and the dynamics of deserts. *Quarterly Journal of the Royal Meteorological Society* 122: 1385–1404.
- Rubio JL (2009) Desertification and water scarcity as a security challenge in the Mediterranean. In: Rubio JL, Safriel U, Daussa R and et al. (eds) *Water Scarcity, Land Degradation and Desertification in the Mediterranean Region*. Dordrecht: Springer, pp. 75–92.
- Schneider U, Becker A, Finger P et al. (2011) GPCC full data reanalysis version 6.0 (at 1.0°): Monthly land-surface precipitation from rain-gauges built on GTS-based and historic data. Available at: http://dx.doi.org/10.5676/DWD_GPCC/FD_M_V6_050.
- Schneider U, Becker A, Finger P et al. (2013) GPCC's new land surface precipitation climatology based on quality-controlled in situ data and its role in quantifying the global water cycle. *Theoretical and Applied Climatology*. Epub ahead of print 20 March. DOI: 10.1007/s00704-013-0860-x.
- Sowers J, Vengosh A and Weinthal E (2011) Climate change, water resources, and the politics of adaptation in the Middle East and North Africa. *Climatic Change* 104: 599–627.
- Stokes MA and Smiley TL (1996) *An Introduction to Tree-Ring Dating*. Chicago, IL: University of Chicago Press.
- Tibshirani R, Walther G and Hastie T (2001) Estimating the number of clusters in a data set via the gap statistic. *Journal of the Royal Statistical Society Series B: Statistical Methodology* 63(2): 411–423.
- Touchan R, Meko DM and Aloui A (2008a) Precipitation reconstruction for northwestern Tunisia from tree ring. *Journal of Arid Environments* 72: 1887–1896.
- Touchan R, Meko DM and Hughes MK (1999) A 396-year reconstruction of precipitation in southern Jordan. *Journal of the American Water Resources Association* 35: 45–55.
- Touchan R, Akkemik Ü, Hughes MK et al. (2007) May–June precipitation reconstruction of south-western Anatolia, Turkey during the last 900 years from tree rings. *Quaternary Research* 68(2): 196–202.
- Touchan R, Anchukaitis KJ, Meko DM et al. (2008b) The long term context for recent drought in northwestern Africa. *Geophysical Research Letters* 35: L13705.
- Touchan R, Anchukaitis KJ, Meko DM et al. (2011) Spatiotemporal drought variability in northwestern Africa over the last nine centuries. *Climate Dynamics* 37: 237–252.
- Touchan R, Funkhouser G, Hughes MK et al. (2005a) Standardized precipitation indices reconstructed from Turkish tree-ring widths. *Climatic Change* 72(3): 339–353.
- Touchan R, Garfin GM, Meko DM et al. (2003) Preliminary reconstructions of spring precipitation in southwestern Turkey from tree-ring width. *International Journal of Climatology* 23: 157–171.
- Touchan R, Shishov VV, Meko DM et al. (2012) Process based model sheds light on climate signal of Mediterranean tree-ring width. *Biogeosciences* 9: 965–972.
- Touchan R, Xoplaki E, Funkhouser G et al. (2005b) Dendroclimatology and large-scale circulation influences in the eastern Mediterranean and near east region. *Climate Dynamics* 25: 75–98.
- Trigo IF, Davies TD and Bigg GR (1999) Objective climatology of cyclones in the Mediterranean region. *Journal of Climate* 12: 1685–1696.
- Van der Schrier G, Barichivich J, Briffa KR et al. (2013) A scPDSI-based global data set of dry and wet spells for 1901–2009. *Journal of Geophysical Research: Atmospheres* 118: 4025–4048.
- Wigley TML, Briffa KR and Jones PD (1984) On the average value of correlated time series, with applications in dendroclimatology and hydrometeorology. *Journal of Climate and Applied Meteorology* 23: 201–213.
- Xoplaki E, Maheras P and Luterbacher J (2001) Variability of climate in meridional Balkans during the periods 1675–1715 and 1780–1830 and its impact on human life. *Climatic Change* 48: 581–615.
- Xoplaki E, González-Rouco JF, Gyalistras D et al. (2003a) Inter-annual summer air temperature variability over Greece and its connection to the large scale atmospheric circulation and Mediterranean SSTs 1950–1999. *Climate Dynamics* 20: 537–554.
- Xoplaki E, González-Rouco JF, Luterbacher J et al. (2003b) Mediterranean summer air temperature variability and its connection to the large scale atmospheric circulation and SSTs. *Climate Dynamics* 20: 723–739.
- Xoplaki E, González-Rouco JF, Luterbacher J et al. (2004) Wet season Mediterranean precipitation variability: Influence of large-scale dynamics and predictability. *Climate Dynamics* 23: 63–78.
- Xoplaki E, Luterbacher J, Paeth H et al. (2005) European spring and autumn temperature variability and change of extremes over the last half millennium. *Geophysical Research Letters* 32: L15713.